Online Supporting Information for

Gas-particle partitioning of primary organic aerosol emissions: (2) diesel vehicle exhaust

Andrew A. May, Albert A. Presto, Christopher J. Hennigan, Ngoc T. Nguyen, Timothy D. Gordon, Allen L. Robinson[1]

Center for Atmospheric Particle Studies, Carnegie Mellon University, Pittsburgh PA

[1] Corresponding author alr@andrew.cmu.edu, current address Dept. of Mechanical Engineering, Carnegie Mellon University, Pittsburgh, PA

Schematic of experimental setup

Here, we provide the experimental setup for emissions testing of the diesel vehicles in this study. Emissions were collected from the source during the chassis dynamometer cycle and diluted in a constant volume sampler (CVS). The average dilution factor (calculated with Equation S1 defined below) in the CVS was ~20 for the UC and UDDS, ~10 for the HHDDT, and ~100 for C/I. Filter samples were collected from the CVS for off-line organic and elemental carbon analysis as well as thermal desorption-gas chromatography-mass spectrometry analysis. Emissions were also drawn from the CVS into the Carnegie Mellon University portable environmental chamber where they were analyzed using a thermodenuder in conjunction with a quadrupole aerosol mass spectrometer for composition (AMS; Aerodyne Research, Inc., Billerica, MA) and a scanning mobility particle sizer for particle size distributions (SMPS; TSI, Inc., Shoreview, MN).

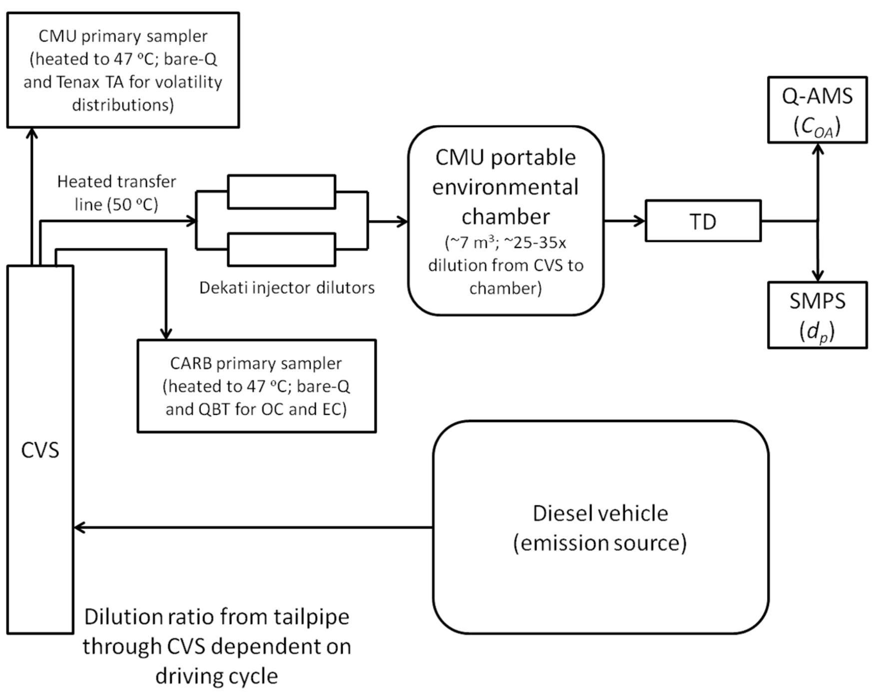

Figure S1. Experimental setup for emissions testing. Emissions from the diesel vehicles were drawn into the CVS, where the emissions were diluted based on the driving cycle. Samples were collected from the CVS onto bare-Q filter and QBT filters, and into the CMU portable environmental chamber. Emissions were diluted further by a factor of ~25-35 from the CVS to the chamber.

Vehicle information

Table S1 provides a list of all vehicles investigated in the present work, sorted by vehicle. Table S2 provides the driving cycle and fuel type, as well as EF_Q, EF_{EC}, and vehicle fuel economy for each vehicle tested.

Table S1. Summary of diesel vehicles tested.

Vehicle ID	Model year	Mileage	After-treatment	Engine displacement (L)	Average fuel economy (mpg)
D1	2010	11,000	DOC+DPF+SCR	14.9	4.5
D2	2007	22,000	DOC+DPF	12.8	4.9
D3	2006	94,000	none	10.8	4.3
D4	2005	66,000	DOC	6.6	11.8
D5	2001	159,000	none	5.9	13.7

DOC = diesel oxidative catalyst; DPF = diesel particulate filter; SCR = selective catalytic reduction

Table S2. Summary of experimental conditions for each test and the resultant emission values.

Vehicle ID	Test ID	Driving cycle	Fuel type	Dilution ratio	CVS temperature (°C)	Filter temperature (°C)	EF_Q (mg kg fuel^{-1})	EF_{QBT} (mg kg fuel^{-1})	C_{OA} (μg m^{-3})	EF_{EC} (mg kg fuel^{-1})
D1[@]	1458	2xUDDS	9%A	15.6	50.3	47.6	4.9	3.4	6.7	n/a
D1[@]	1461	2xUDDS	9%A	15.5	51.4	47.8	6.4	3.9	12.1	0.9
D1[@]	1455	2xUDDS	12%A	15.5	50.8	47.1	4.7	3.7	4.8	n/a
D1[@]	1452	2xUDDS	12%A	15.7	49.9	47.7	7.9	5.7	10.9	1.0
D2[@]	1427	3xcruise	12%A	7.4	91.1	47.0	7.0	1.0	62.0	0.4
D2[@]	1426	3xcruise	12%A	7.5	86.1	46.9	7.2	3.7	35.9	n/a
D2[@]	1418	2xUDDS	12%A	16.8	51.1	47.6	5.2	3.5	7.4	0.5
D2[@]	1413	2xUDDS	12%A	17.0	50.6	47.7	11.3	11.0	1.2	1.8
D3	1439	C/I	28%A	96.8	31.1	46.9	589	181	321	102.1
D3	1443	C/I	9%A	98.2	31.3	46.8	318	155	126	68.0
D3	1436	C/I	12%A	97.5	29.7	46.8	286	133	120	96.7
D3[*,#]	1434	C/I	12%A	96.8	29.5	46.7	388	136	198	96.7
D3	1440	3xcruise	28%A	9.6	80.1	47.1	82.7	18.6	507	191.8
D3	1444	3xcruise	9%A	9.9	80.7	46.9	69.7	19.0	390	177.3
D3	1435	3xcruise	12%A	9.8	79.6	46.9	70.2	15.1	427	166.9
D3	1437	3xcruise	12%A	9.7	78.1	46.9	73.8	16.8	445	169.9
D3[*,#]	1441	2xUDDS	28%A	17.2	52.0	47.8	79.1	26.2	235	210.0
D3[*,#]	1433	2xUDDS	28%A	17.3	52.6	47.8	83.6	28.3	248	226.7
D3[*,#]	1445	2xUDDS	9%A	17.5	55.7	47.7	76.6	23.2	232	220.2
D3[*,#]	1442	2xUDDS	9%A	17.6	53.0	48.1	84.5	30.7	233	203.6
D3[*,#]	1432	2xUDDS	12%A	17.2	55.4	46.9	76.7	20.7	249	265.3

Vehicle ID	Test ID	Driving cycle	Fuel type	Dilution ratio	CVS temperature (°C)	Filter temperature (°C)	EF_Q (mg kg fuel^{-1})	EF_{QBT} (mg kg fuel^{-1})	C_{OA} (μg m^{-3})	EF_{EC} (mg kg fuel^{-1})
D3*,#	1438	2xUDDS	12%A	17.0	53.6	47.6	80.2	23.9	248	214.9
D4*,#	1027980	UC	12%A	22.2	30.7	46.0	156.6	18.1	487	610.1
D4*	1027980	UC	12%A	21.9	29.3	46.8	67.0	14.6	187	242.0
D5#	1028080	UC	12%A	26.9	31.0	46.1	110.1	24.0	249	199.2

* Isothermal dilution data; # Thermodenuder data

@: DPF-equipped vehicle

12%A: CARB ultralow sulfur diesel (ULSD); 9%A: 9% low aromatic ULSD; 28%A: Federal B 28% aromatic ULSD

UDDS: Urban dynamometer driving schedule; HHDDT: Heavy heavy-duty diesel truck cruise;

C/I: Creep/idle driving; UC: Unified cycle (LA-92)

Driving cycle descriptions

For the UDDS tests, two cycles were performed consecutively following a warm-up and hot soak period in order to increase sampling time/resolution. The HHDDT cruise cycle is primarily a steady-state driving cycle at ~55 mph for ~20 minutes, with a transient period at the beginning and end of the cycles. Three HHDDT high speed cruise modes were tested back to back. The creep cycle is a 4 minute transient cycle at low speed (< 10 mph). Three creep cycles were performed in series followed by a 30 minute idling period. From here on, this 3x creep + 30 minute idle cycle will be referred to as C/I while the 3x cruise cycle will be referred to as HHDDT. These driving cycles are summarized in Table S3.

Table S3. Summary of driving cycles.

Parameter	UC	UDDS	HHDDT cruise	HHDDT creep
Average speed, km/hr	39.7	30.3	64.4	2.9
Stops/km	0.9	1.6	0.2	15.0
Max. speed, km/hr	108.4	93.5	95.6	13.3
Max. accel., km/hr/s	11.1	7.1	3.7	3.7
Max. decel., km/hr/s	-14.2	-7.4	-4.0	4.1
Percent idle	16.4	33.4	8.0	42.29*

* Percent idle in HHDDT creep cycle

Fuel composition

Diesel experiments were performed using one of three ultralow sulfur diesel fuels: low aromatic (9% aromatic content), mid-aromatic (12% aromatic content) and high aromatic (28% aromatic content). Fuels were analyzed at a commercial laboratory (Triton Analytics, Houston, TX) using nitric oxide ionization spectrometry evaluation (NOISE). NOISE quantifies hydrocarbons by carbon number and hydrogen deficiency (Villalanti and Wadsworth, 1993). In addition to measuring the mono-, di-, tri-, and tetra-aromatic content, this gas chromatography/mass spectrometry (GC/MS) technique provides the weight percentages of ten other classes of compounds. Basic composition data of the three fuels used with the HDDVs are provided in Table S4.

Table S4. Diesel fuel composition analysis.

Component	low aromatic	mid aromatic	high aromatic
Alkanes (wt %)	19.9	26.4	29.3
Cycloalkanes (wt %)	70.9	61.2	42.7
Mono-aromatics (wt %)	8.8	11.7	23.7
Di-aromatics (wt %)	0.4	0.7	4.2
Tri-aromatics (wt %)	0.0	0.0	0.2
Tetra-aromatics (wt %)	0.0	0.0	0.0
Average # carbons	15.0	14.1	14.7
Average H/C	1.9	1.9	1.8
Average O/C	0.0	0.0	0.0
Average molecular weight (g/mol)	208.5	196.7	203.7

Dilution ratio

The dilution ratios reported in Tables S1 and S2 were calculated following the approach of Lipsky and Robinson [2006]:

$$DR = \frac{[CO_2]_{ex} - [CO_2]_{bkd}}{[CO_2]_{tun} - [CO_2]_{bkd}} \qquad (S1)$$

where subscripts *ex*, *bkd*, and *tun* represent the missing ratio of CO_2 in the exhaust (at the tailpipe), background air, and CVS, respectively. Background and CVS concentrations of CO_2 were directly measured during each test. Exhaust CO_2 concentrations were calculated assuming stoichiometric combustion:

$$C_nH_m + \left(n + \frac{m}{4}\right)(O_2 + 3.76N_2) \rightarrow nCO_2 + \frac{m}{2}H_2O + 3.76\left(n + \frac{m}{4}\right)N_2 \qquad (S2)$$

We obtain subscripts *n* and *m* from fuel analysis to be 7.08 and 15, respectively (fuel is 85% carbon by mass). We then calculate the mixing ratio of CO_2 in the exhaust as:

$$\% \, CO_2 = \frac{n}{n + \frac{m}{2} + 3.76\left(n + \frac{m}{4}\right)} \quad (S3)$$

Equilibrium timescales

To assess whether aerosol has reached phase equilibrium, it is necessary to calculate the equilibrium timescale τ, which can be approximated as the inverse of the condensation sink (CS) [*Seinfeld and Pandis*, 2006]:

$$\tau = CS^{-1} = \left(2\pi d_p N_t D F\right)^{-1} \quad (S4a)$$

$$F = \frac{1 + Kn}{1 + 0.3773Kn + 1.33Kn\frac{1 + Kn}{\alpha}} \quad (S4b)$$

where d_p is the mass-median particle size (assumed monodisperse), N_t is the total aerosol number concentration, D is the diffusion coefficient for the organic vapors in air (assumed to be 5 x 10^{-6} m^2 s^{-1} [*Riipinen et al.*, 2010]), and F is the Fuchs-Sutugin correction factor, which accounts for non-continuum effects. Kn is the Knudsen number (= $2\lambda/d_p$, where λ = 65.2 nm, the mean free path of organic molecules in air at 1 atm and 25 °C), and α is the mass accommodation coefficient. Saleh et al. [2011] recommend that a system should be treated as equilibrium only if the ratio of the residence time in the system to τ is greater than 5.

Effects of experimental conditions

Different combinations of vehicles, driving cycles, and fuel type were considered during this study. Figure S2 re-plots Figure 2 to investigate any systematic biases caused by differences in the test. Clearly, there is no systematic trend in the data due to different driving cycles, vehicles, or fuel types. From Figure S2, it is also evident a volatility distribution derived from used lubricating oil systematically over-predicts the experimental data, while a volatility distribution derived from the exhaust that assumes the TD-GC-MS is missing extremely-low-volatility material ($C_i^* < 3 \times 10^{-4}$ μg m^{-3}) does not capture the correct trend in the data.

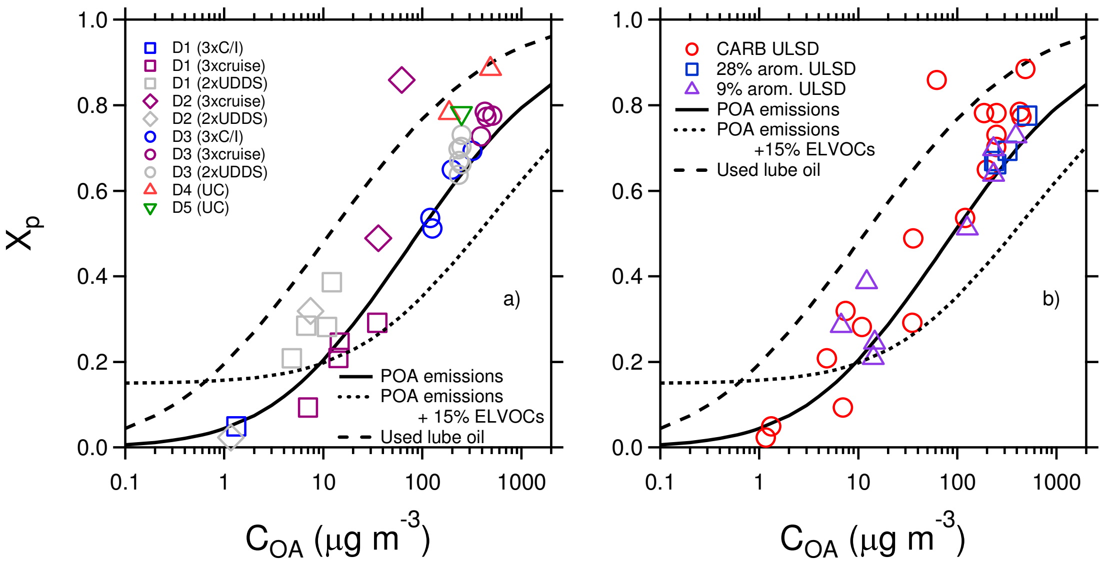

Figure S2. Partitioning plot of the data presented in Figure 1. **a)** Comparing differences between vehicles and driving cycle. **b)** Comparing differences between fuel types. There is no obvious bias due to different experimental conditions. The solid line represents the model prediction using the median volatility distribution from the TD-GC-MS method, while the dashed line represents the volatility distribution derived using the TD-GC-MS method for used lubricating oil. The dotted line represents a model assuming there is 15% EVLOCs in the volatility distribution that the TD-GC-MS cannot characterize. Model predictions are performed at $T = 47$ °C.

Figures S3 compares predicted partitioning for different driving cycles and fuels to the prediction made by the median volatility distribution for all POA emissions. These predictions are based on the TD-GC-MS data. Figure S3a considers the effects of driving cycle, while Figure S3b considers fuel type. Predictions for the different conditions fall very near the 1:1 line (markers), suggesting that the volatility distributions of the POA emissions are not sensitive to driving cycles and fuel composition, corroborating the finding from Figure S3. In Table S4, we provide volatility distributions derived for each test.

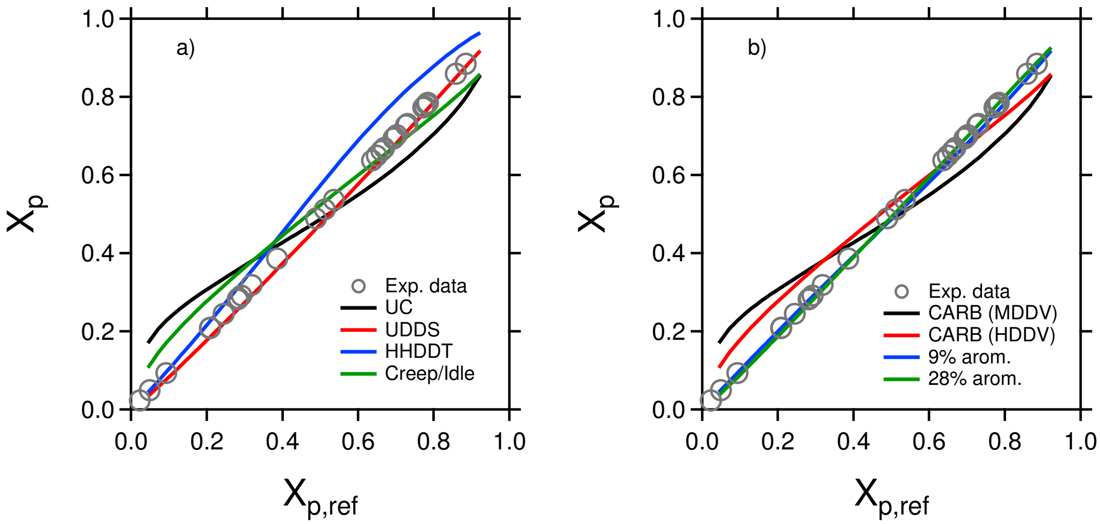

Figure S3. Considering the effect of **a)** different driving cycles and **b)** different fuel types on model predictions (i.e., on volatility distributions).

Table S5. Volatility distributions derived for all vehicle tests.

Vehicle ID	Test ID	Driving cycle	Fuel type	10^{-2}	10^{-1}	10^{0}	10^{1}	10^{2}	10^{3}	10^{4}	10^{5}	10^{6}
D1[@]	1448	UDDS	28%A	0.00	0.04	0.14	0.39	0.24	0.08	0.04	0.04	0.05
D1[@]	1450	C/I	28%A	0.00	0.02	0.06	0.29	0.26	0.10	0.07	0.12	0.10
D1[@]	1452	UDDS	12%A	0.00	0.01	0.11	0.40	0.27	0.07	0.03	0.05	0.06
D1[@]	1453	HHDDT	12%A	0.00	0.04	0.33	0.48	0.11	0.03	0.01	0.00	0.01
D1[@]	1456	C/I	12%A	0.00	0.02	0.14	0.30	0.23	0.09	0.06	0.08	0.08
D1[@]	1458	UDDS	9%A	0.00	0.02	0.10	0.34	0.25	0.09	0.05	0.08	0.07
D2[@]	1407	UDDS	28%A	0.00	0.02	0.10	0.56	0.19	0.05	0.03	0.02	0.02
D2[@]	1413	UDDS	12%A	0.01	0.03	0.10	0.44	0.27	0.07	0.04	0.03	0.03
D2[@]	1418	UDDS	12%A	0.01	0.02	0.07	0.36	0.32	0.07	0.06	0.04	0.06
D2[@]	1420	C/I	12%A	0.01	0.03	0.09	0.30	0.29	0.08	0.07	0.06	0.07
D2[@]	1426	HHDDT	12%A	0.00	0.02	0.20	0.53	0.221	0.02	0.00	0.00	0.02
D3	1433	UDDS	12%A	0.07	0.22	0.35	0.22	0.08	0.03	0.02	0.01	0.00
D3	1436	C/I	12%A	0.06	0.18	0.29	0.26	0.11	0.05	0.03	0.01	0.00
D3	1439	C/I	28%A	0.06	0.20	0.33	0.25	0.11	0.03	0.01	0.00	0.00
D3	1444	C/I	9%A	0.06	0.22	0.34	0.21	0.09	0.05	0.02	0.01	0.00
D3	1445	UDDS	9%A	0.00	0.01	0.26	0.35	0.26	0.08	0.03	0.01	0.01
D3	1442	UDDS	9%A	0.00	0.03	0.23	0.33	0.28	0.08	0.03	0.01	0.01
D3	1432	UDDS	12%A	0.00	0.01	0.29	0.38	0.23	0.05	0.02	0.01	0.01
D3	1433	UDDS	12%A	0.00	0.02	0.29	0.38	0.22	0.05	0.03	0.01	0.01

Vehicle ID	Test ID	Driving cycle	Fuel type	10^{-2}	10^{-1}	10^{0}	10^{1}	10^{2}	10^{3}	10^{4}	10^{5}	10^{6}
D3	1438	UDDS	28%A	0.00	0.01	0.26	0.38	0.25	0.06	0.03	0.01	0.00
D3	1441	UDDS	28%A	0.00	0.00	0.25	0.37	0.28	0.06	0.03	0.01	0.01
D3	1435	HHDDT	12%A	0.01	0.09	0.27	0.38	0.18	0.03	0.02	0.01	0.01
D3	1437	HHDDT	12%A	0.01	0.10	0.28	0.38	0.19	0.03	0.01	0.01	0.01
D3	1440	HHDDT	28%A	0.01	0.09	0.24	0.37	0.23	0.03	0.01	0.01	0.00
D3	1444	HHDDT	9%A	0.01	0.10	0.31	0.36	0.16	0.04	0.01	0.01	0.00
D4	1027980	UC	12%A	0.00	0.11	0.16	0.21	0.25	0.17	0.08	0.02	0.01
D4	1028019	UC	12%A	0.22	0.12	0.13	0.18	0.16	0.11	0.06	0.02	0.01
Median lubricating oil	n/a	n/a	n/a	0.24	0.20	0.15	0.19	0.14	0.04	0.02	0.01	0.01

[@]: DPF-equipped vehicle
12%A: CARB ultralow sulfur diesel; 9%A: 9% low aromatic ULSD;
28%A: Federal B 28% aromatic ULSD
UDDS: Urban dynamometer driving schedule; HHDDT: Heavy heavy-duty diesel truck cruise;
C/I: Creep/idle driving; UC: Unified cycle (LA-92)

Experimental data

Here, we provide data tables of the dilution measurements found in Figures 2 and 3 (Table S5) as well as the thermodenuder measurements found in Figure 4 (Table S6).

Table S6. Dilution data presented in Figures 3 and 4 in the main text.

Vehicle ID	Test ID	EF_{OA} (CVS) (mg kg-fuel^{-1})	Dilution ratio (CVS)	X_p (CVS)	EF_{OA} (chamber) (mg kg-fuel^{-1})	Dilution ratio (chamber)	X_p (chamber)
D4	1027980	139	22.2	0.88	0.3	35.6	0.06
D4	1028019	52.3	21.9	0.78	0.8	30.5	0.38
D3	1445	53.4	17.5	0.70	0.8	29.8	0.32
D3	1432	56.1	17.2	0.73	2.1	26.4	0.71
D3	1441	52.9	17.2	0.67	1.1	29	0.39
D3	1443	56.3	98.2	0.70	0.9	33.6	0.38
D3	1438	55.3	17.0	0.66	1.2	29.6	0.41
D3	1442	53.9	17.6	0.64	0.9	30.3	0.31
D3	1436	154	97.5	0.54	0.6	29.3	0.06

Table S7. Thermodenuder data presented in Figure 5 in the main text.

Vehicle ID	Test ID	C_{OA} (μg m^{-3})	dp (nm)	*MFR* (25 °C)	*MFR* (40 °C)	*MFR* (80 °C)	*MFR* (100 °C)	*MFR* (120 °C)
D4	1027980	0.9	191	n/a	0.96	0.58	n/a	0.56
D3	1432	9.1	267	0.90	0.6	0.49	0.50	n/a
D3	1443	4.0	253	0.68	1.0	1.0	0.87	n/a
D3	1438	5.2	266	0.88	1.0	0.80	0.70	n/a
D3	1441	4.8	245	0.86	0.67	0.76	0.62	n/a
D3	1442	3.8	247	1.0	0.69	0.85	0.41	n/a
D3	1445	3.6	253	0.96	0.60	0.77	0.74	n/a
D5	1028080	5.3	170	n/a	0.70	0.54	n/a	0.64

Modeling thermodenuder data

For dynamic systems, a kinetic equation must be applied, tracking both particle- and gas-phase concentrations of each volatility bin *i*:

$$\frac{dC_{p,i}}{dt} = -2\pi d_p N_t DF\left(X_{m,i} Ke C_i^* - C_{g,i}\right) \quad (S5a)$$

$$\frac{dC_{g,i}}{dt} = -\frac{dC_{p,i}}{dt} \quad (S5b)$$

where $C_{p,i}$ is the particle-phase mass concentration of *i*, d_p is the particle diameter, *D* is the diffusion coefficient of particles in air, and $C_{g,i}$ is the gas-phase mass concentration. $X_{m,i}$ is the mass fraction of *i* in the particle phase. *F* is the Fuchs-Sutugin correction term and *Ke* represents the Kelvin effect:

$$F = \frac{1 + Kn}{1 + 0.3773Kn + 1.33Kn\left(\frac{1 + Kn}{\alpha}\right)} \quad (S6)$$

$$X_{m,i} = \frac{f_i C_{tot}}{C_{OA}}\left(1 + \frac{C_i^*(T)}{C_{OA}}\right)^{-1} \quad (S7)$$

$$Ke = \exp\left(\frac{4\sigma MW_i}{\rho RT d_p}\right) \quad (S8)$$

where Kn is the Knudsen number ($2\lambda/d_p$), α is the mass accommodation coefficient, σ is the surface tension of the bulk particle, MW_i is the molecular weight of $_i$, ρ is the density of the bulk particle, R is the ideal gas constant, and T is the temperature. We make assumptions on the values of D, MW_i, σ, and ρ based on Riipinen et al. [*Riipinen et al.*, 2010]. C_i^* will vary with temperature following the Clausius-Clapeyron equation:

$$C_i^*(T) = C_i^*(298\ K)\exp\left[-\frac{\Delta H_{vap,i}}{R}\left(\frac{1}{T} - \frac{1}{298\ K}\right)\right]\frac{298\ K}{T} \quad (S9)$$

where $\Delta H_{vap,i}$ is the enthalpy of vaporization of i.

All model inputs are known from a priori knowledge or experimental measurements. Since chamber C_{OA} and d_p were similar in all experiments, the median values were used as inputs to the model, along with volatility distributions from TD-GC-MS analysis which are used to define all species i. Values of ΔH_{vap} from Ranjan et al. [2012] are assumed as well as a mass accommodation coefficient (α) of unity. Values of important parameters are summarized in Table S7.

Table S8. Parameters used in evaporation kinetics model.

Parameter	Value
Diffusion coefficient[a], D	5×10^{-6} m^2 s^{-1}
Surface tension[a], σ	0.05 N m^{-1}
Particle bulk density[b], ρ	1200 kg m^{-3}
Molecular weight[c], MW_i	$0.434 - 0.045 \log C_i^*$
Volatility basis set, C_i^*	10^{-2}, 10^{-1}, 10^0, 10^1, 10^2, 10^3, 10^4, 10^5, 10^6
Enthalpy of vaporization, $\Delta H_{vap,i}$[d]	$85 - 11 \log C_i^*$
Mass accommodation coefficient, α	1

a based on Riipinen et al. [2010]; *b* based on Lee et al. [2010]; *c* based on values for *n*-alkanes; *d* based on Ranjan et al. [2012]

The effect of reducing α has been investigated to explore the poor agreement between measured and modeled TD data. Reducing α to 0.1 or 0.01 merely slows down the evaporation kinetics, while retaining the same overall shape of the curve (Figure S4). However, the curve that best approximates the data is represented by the curved line with the shallower slope, which may be an approximation for a predictive model assuming *ad*sorption is influencing gas-particle partitioning in the TD. Development of such a model is outside the scope of the current work.

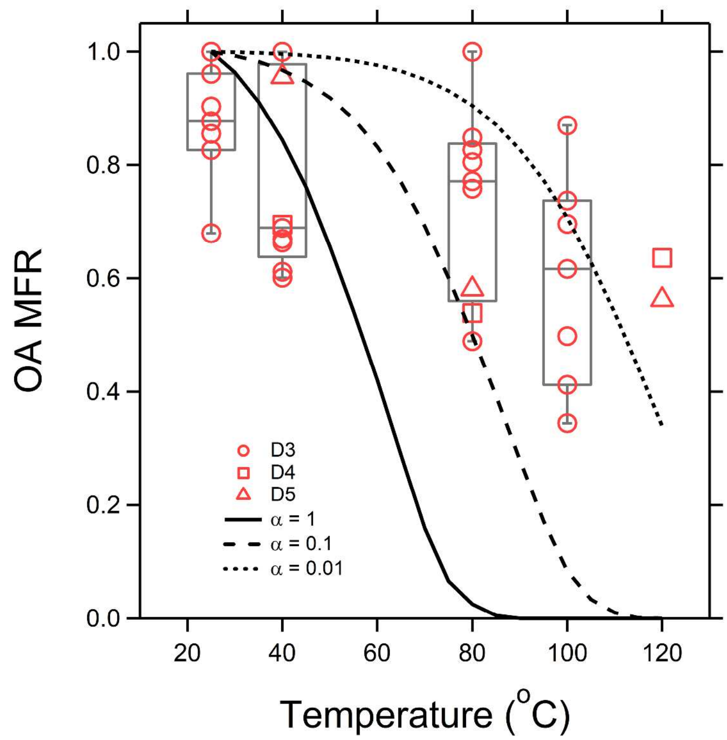

Figure S4. Investigating the effects of the mass accommodation coefficient (α). Reducing α from unity does not reasonably predict the experimental data, suggesting that adsorption may be playing an important role in the gas-particle partitioning of the diesel POA emissions in the TD.

Comparison to previous studies

Our research group has extensively characterized the POA emissions from a small diesel generator [*Grieshop et al.*, 2009; *Lipsky and Robinson*, 2006; *Ranjan et al.*, 2012; *Shrivastava et al.*, 2006]. Here, we provide a comparison between the current work and parameterizations from previous work. Prior results all agree reasonably well with each other as they are all derived from the same source. However, the predictions based on previous work all predict POA that is more volatile than was observed for diesel vehicles (note that the circles in Figure S5 represent filter data collected at 47°C while the model predictions are based on 25 °C).

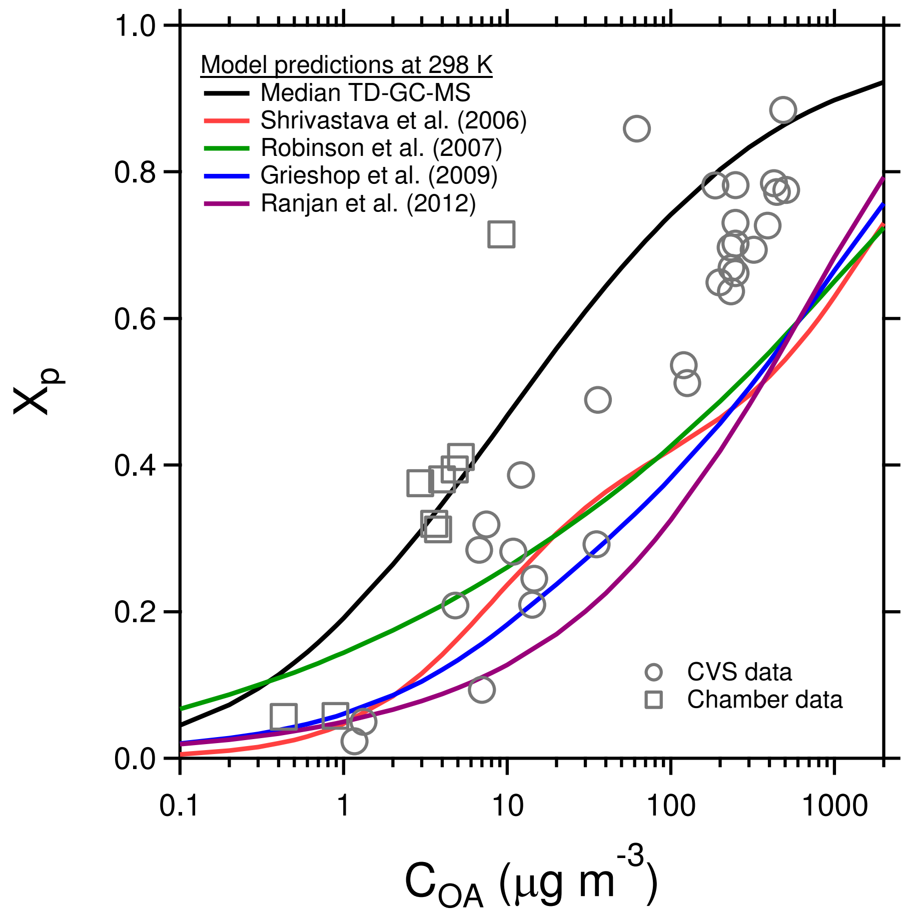

Figure S5. Comparison of model predictions from the current study and prior work.

References

Grieshop, A. P., N. M. Donahue, and A. L. Robinson (2009), Laboratory investigation of photochemical oxidation of organic aerosol from wood fires 2: analysis of aerosol mass spectrometer data, *Atmos Chem Phys*, *9*(6), 2227-2240.

Lee, B. H., et al. (2010), Measurement of the ambient organic aerosol volatility distribution: application during the Finokalia Aerosol Measurement Experiment (FAME-2008), *Atmos Chem Phys*, *10*(24), 12149-12160.

Lipsky, E. M., and A. L. Robinson (2006), Effects of dilution on fine particle mass and partitioning of semivolatile organics in diesel exhaust and wood smoke, *Environmental Science & Technology*, *40*(1), 155-162.

Ranjan, M., A. A. Presto, A. A. May, and A. L. Robinson (2012), Temperature Dependence of Gas-Particle Partitioning of Primary Organic Aerosol Emissions from a Small Diesel Engine, *Aerosol Sci Tech*, *46*(1), 13-21.

Riipinen, I., J. R. Pierce, N. M. Donahue, and S. N. Pandis (2010), Equilibration time scales of organic aerosol inside thermodenuders: Evaporation kinetics versus thermodynamics, *Atmos Environ*, *44*(5), 597-607.

Shrivastava, M. K., E. M. Lipsky, C. O. Stanier, and A. L. Robinson (2006), Modeling semivolatile organic aerosol mass emissions from combustion systems, *Environmental Science & Technology*, *40*(8), 2671-2677.